

## Mono- and multi-layer adsorption of an ionic liquid on Au(110)

Richard Foulston<sup>1</sup>, Subhashis Gangopadhyay<sup>2</sup>, Cristina Chiutu<sup>2</sup>,  
Philip Moriarty<sup>2</sup>, and Robert G Jones<sup>1\*</sup>

<sup>1</sup> Department of Physical Chemistry  
School of Chemistry  
University of Nottingham  
Nottingham NG7 2RD

<sup>2</sup> School of Physics and Astronomy  
University of Nottingham  
Nottingham NG7 2RD

### Supplementary Information

References for the Supplementary Information are listed at the end of the document.

### Evaporator

[C<sub>2</sub>C<sub>1</sub>Im][Tf<sub>2</sub>N], was adsorbed onto the Au(110) surface by vapour phase deposition from a purpose-built evaporator. The evaporator consisted of a heated 10 ml glass vial charged with  $\approx$  1 ml of [C<sub>2</sub>C<sub>1</sub>Im][Tf<sub>2</sub>N]. The glass vial was enclosed in a copper tube that was heated by a 12 V, 20 W tungsten halogen light bulb, with temperature measurement using a type K thermocouple. The IL vapour was collimated into a molecular beam using a tube (8 mm diameter x 50 mm long) which could be blocked using a movable baffle. The molecular beam passed through a Bayard Alpert ionization gauge to allow the intensity and stability of the flux to be monitored, before entering the analysis chamber via a gate valve which could be used to isolate the evaporator. For UPS and LEED experiments the entire assembly pointed upwards at an angle of 45° to the horizontal, with a source-to-surface distance of  $\approx$  0.45 m, see Fig. SI 1. For STM experiments the assembly was horizontal, with the glass vial tilted slightly to prevent the IL running out, with a similar source-to-surface distance. Typical operating temperatures for the source were 423–523 K, resulting in a deposition rate of  $0.03 < \theta < 1 \text{ min}^{-1}$  at the sample position, with  $< 10\%$  fluctuation in flux during an experiment. ( $\theta = 1$  corresponds to a monolayer of [C<sub>2</sub>C<sub>1</sub>Im][Tf<sub>2</sub>N] on the Au(110) surface, as determined in this work).

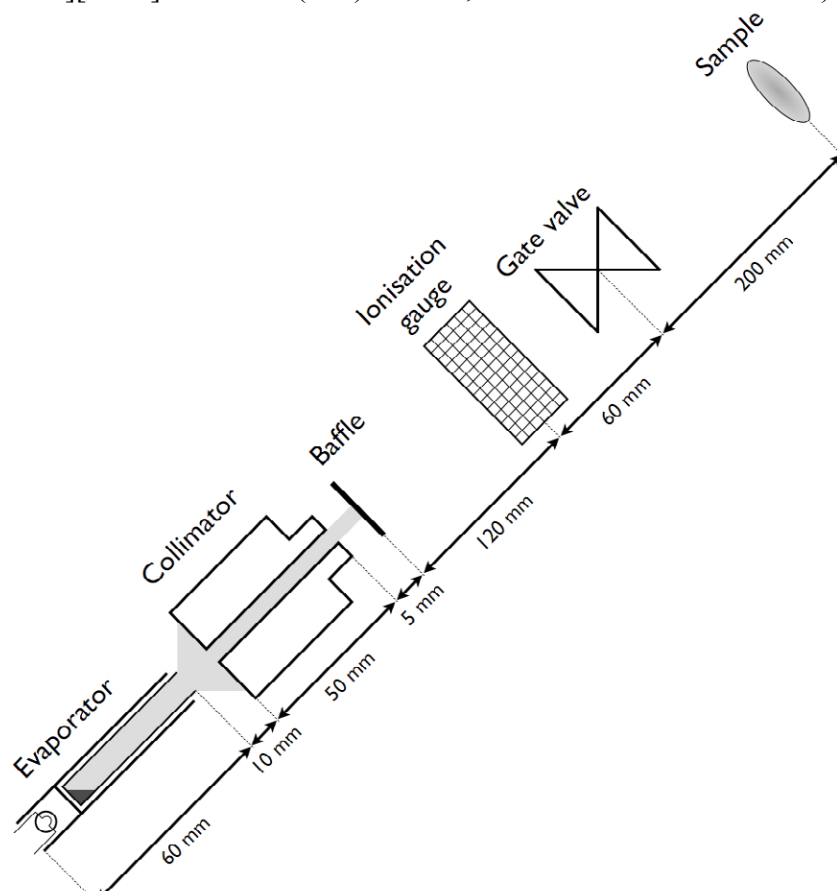


Figure SI 1. Layout and dimensions of the ionic liquid evaporator when used for UPS and LEED experiments.

### Work function measurement

The work function of the substrate was calculated by first finding the difference in energy, A, between the Fermi level position (defined as the energy at half the step height at the Fermi edge) and the secondary electron cut-off (defined as the energy at the half-maximum height of the secondary electron cut off), Fig. SI 2, where  $\phi=21.22\text{-A}$  eV. Where necessary, high resolution UP spectra of the secondary electron region were recorded specifically to get accurate values of the work function.

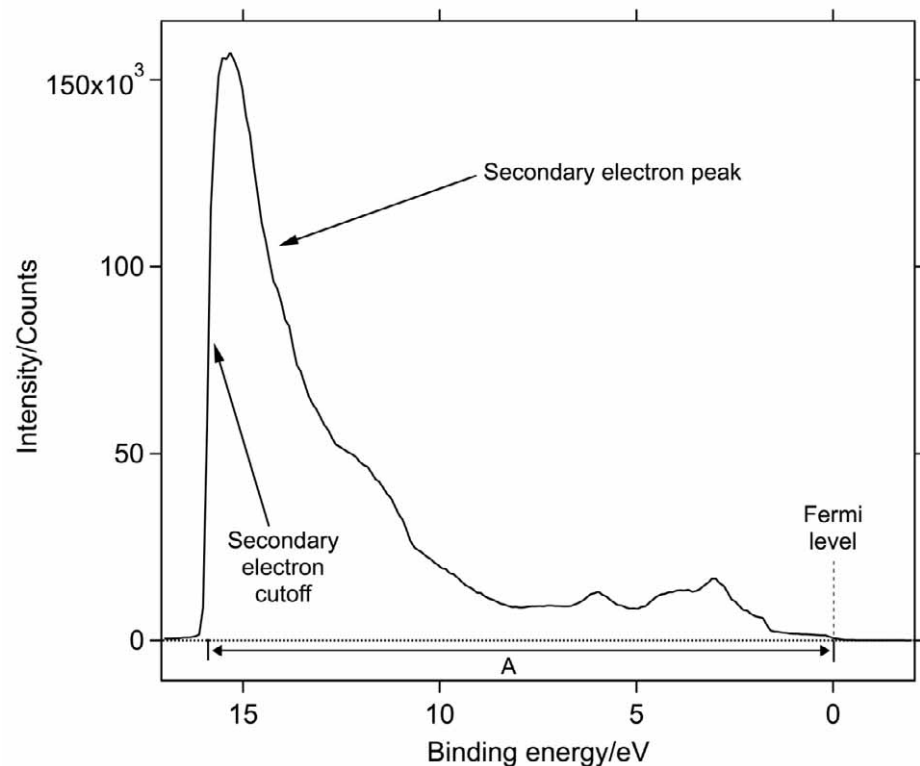


Figure SI 2. UP spectrum of the clean Au(110) substrate, illustrating the energy A.

### Subtraction of clean substrate gold spectrum from the spectra of adsorbate-covered surfaces

UP spectra were taken using a large number of data points and the raw data smoothed using binomial smoothing<sup>1</sup>. For illustration, Fig. SI 3 shows a set of UP spectra for various IL coverages on the Au(110) surface. One of the spectra has been plotted as both the raw data points, and as the smooth curve that was fitted through them. It can be seen that the smooth curve is an accurate representation of the shape of the spectrum. Similar smoothing parameters have been used for all of the spectra in Fig. SI 3, and for all the figures in this work.

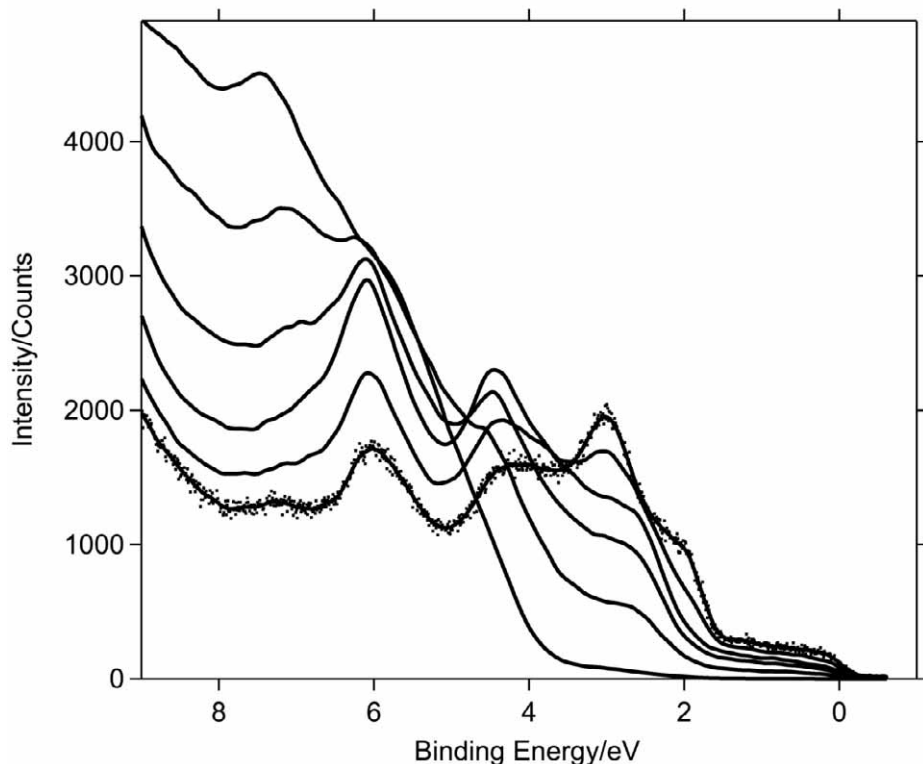


Figure SI 3. UP spectra for various coverages of IL on Au(110). One spectrum (for clean Au(110)) shows the raw data and the smoothed fit, while the other spectra are represented by just the smoothed fit. This illustrates that the essential features of the spectra are retained.

Rather than simply subtracting the clean substrate UP spectrum from the substrate+adsorbate spectra, as is frequently done e.g see Ref. 2 , we adopt a more specific method, allowing the generation of spectra representative of just the adsorbate, and also allowing us to analyse the attenuation of the substrate signal. It can be seen from Fig. SI 3 that all of the IL peaks, and the gold d band and surface states occur at BE  $\gtrsim 2$  eV. Therefore, for  $0 < \text{BE} \lesssim 2$  the spectrum consists solely of photoelectrons emitted from the bulk Au s-band and are representative of the intensity of the bulk gold UP spectrum. We make the assumption that the UP spectrum from an adsorbate-covered surface is a simple summation of an appropriately attenuated bulk Au UP spectrum (as represented by the measured clean surface spectrum) and the IL adsorbate spectrum.

By scaling the measured, clean surface Au UP spectrum, such that its s-band intensity matches the s-band intensity of a measured spectrum for an adsorbate-covered sample in the region  $0 < \text{BE} \lesssim 2$  eV, the scaled clean surface spectrum can be subtracted from the measured spectrum for the

adsorbate-covered surface to leave a spectrum with zero intensity in the  $0 - \approx 2$  eV BE region, representative of just the adsorbed IL. Clearly this procedure assumes no variation in mean free path with electron kinetic energy (which becomes progressively less true for regions of the spectrum that are further from the normalising region of  $0 - \approx 2$  eV BE). Also, surface states on the clean surface are not representative of the bulk substrate spectrum as they collapse, rather than being attenuated, which causes negative peaks, or troughs, in the subtracted spectra for the adsorbed IL. Even with these drawbacks, removal of the bulk substrate spectrum allows a clearer view of the behaviour of the adsorbate peaks. The procedure also provides an estimate of the attenuation of the substrate gold s-band by the overlaying IL layers. Hence, the behaviour of the IL layers with coverage, time and temperature can be deduced using qualitative inelastic mean free path arguments. See main text for specific examples.

The subtraction was performed as follows: an appropriate section of each spectra (unsmoothed) was selected in the gold s band region (typically the region between 0 eV and 1.5 eV BE). The selected part of the clean Au(110) spectrum multiplied by a number N (< 1) was then subtracted from the selected part of the adsorbate covered spectrum to give a difference spectrum. The mean of the sum of the data points in the difference spectrum was then iterated towards zero using a simple algorithm. Typically,  $\approx 150$  data points each carrying about  $\approx 200$  counts were used for the clean surface, giving a total of  $\approx 30000$  counts, and a signal to noise (S/N) of  $\sqrt{30000} = 173$  (less  $\approx 0.6\%$  noise for one sigma). For the adsorbate s band similar intensities occur for high coverages, so the overall noise in the subtracted spectra will be about 1%. As the s band intensity of the adsorbate surface decreases with increasing coverage, the error in the subtracted spectra grows, but even for a 10x reduction in signal (total counts of 3000), the S/N of the adsorbate spectrum is still 55, i.e. a noise level of less than 2%. Consequently, we estimate that the difference spectra (e.g. Figs.3, 9, 13) are reproducible to a few percent for low adsorbate coverages, while the s band intensities of figs. 5, 6, 11, 13 are just one or two percent.

### Clean surface UP spectrum of Au(110)-(1x2)

The UP spectrum for the clean (1x2) reconstructed Au(110) surface, Fig.SI 4, agrees well with spectra in the literature<sup>3,4</sup>, showing two surface states  $S_1$  and  $S_2$ <sup>4</sup>, a broad general intensity for the bulk d band, and a work function of  $5.3 \pm 0.1$  eV, which compares well with the literature value of 5.37 eV<sup>5</sup>.

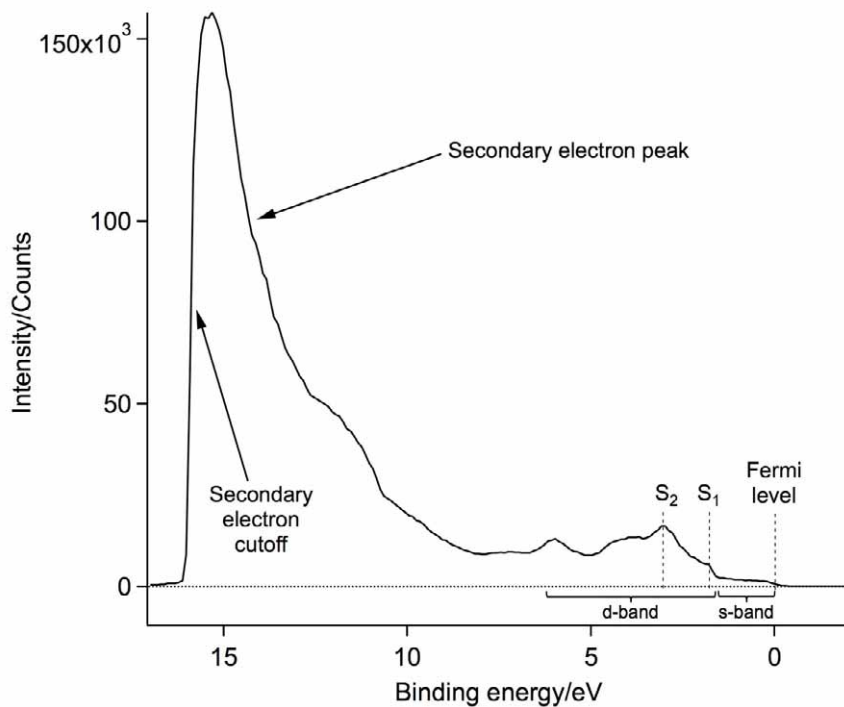


Figure SI 4. He I UP spectrum for the clean Au-(110)-(1x2) reconstructed surface showing the Fermi level, s band and clean surface states  $S_1$  and  $S_2$ .

### UP spectrum of thick layers of $[C_2C_1Im][Tf_2N]$ on Au(110)

Figure SI 5 shows the UP spectrum for multilayers ( $\theta \approx 15$ ) of  $[C_2C_1Im][Tf_2N]$  on the Au(110) surface, while the inset shows the UP spectrum for a macroscopically thick layer of  $[C_2C_1Im][Tf_2N]$  on polycrystalline Au, taken from Ref.<sup>6</sup>. The two spectra agree rather well, indicating that our vapour deposition method successfully deposits the IL without decomposition.

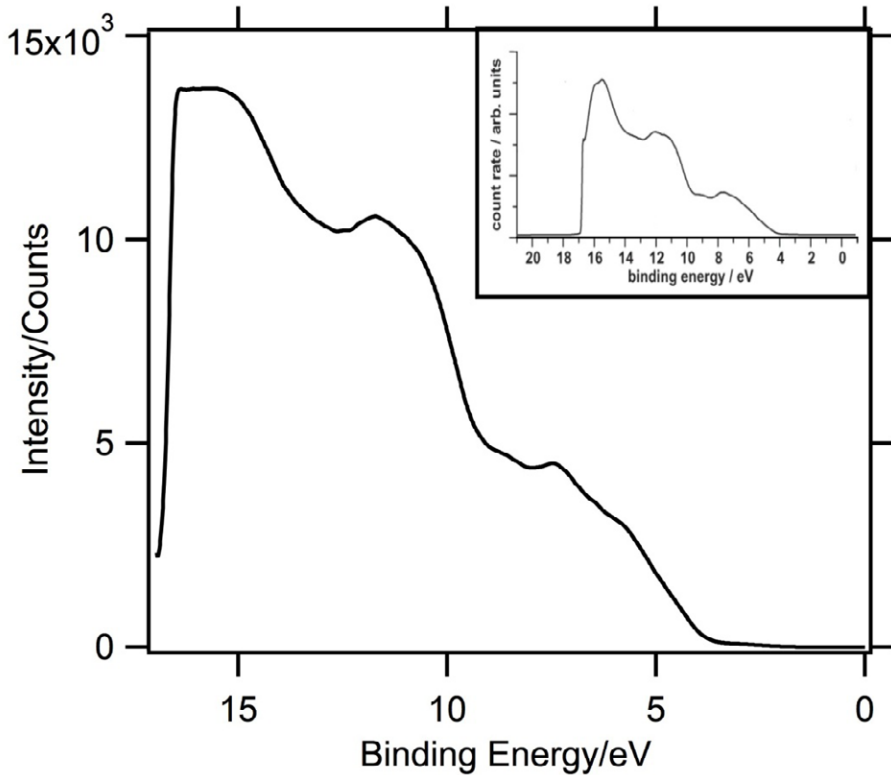


Figure SI 5. UP spectrum of multilayers ( $\theta \approx 15$ ) of  $[C_2C_1Im][Tf_2N]$  on Au(110). The inset shows a UP spectrum recorded by Höfft et al<sup>6</sup> for bulk liquid  $[C_2C_1Im][Tf_2N]$  ( $\approx 1$  mm thickness) on a polycrystalline Au substrate.

### Desorption

Figure SI 6 shows the sequence of UP spectra obtained on annealing a multilayer covered surface ( $\theta \approx 5$ ) to increasingly higher temperatures (each spectrum recorded immediately after heating)

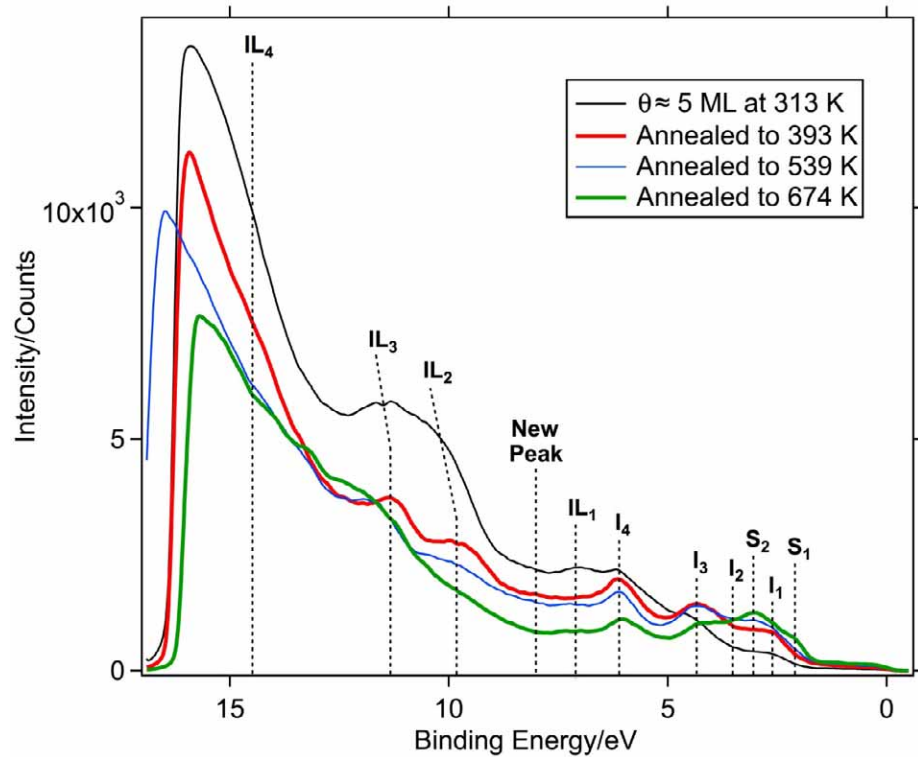


Figure SI 6. UP spectra after annealing a  $\theta \approx 5$  surface to increasingly higher temperatures.

### Adsorption at elevated temperature

Figure SI 7 shows UP spectra for adsorption at 523 K, taken at exposures where  $\phi$  was at its minimum,  $(1\times 3)\text{-}\theta < 1$  structure, and where the coverage had reached the steady state,  $(1\times 1)\text{-}\theta \approx 1$  structure. Also shown is the spectrum for the  $(1\times 1)\text{-}\theta = 1$  structure, formed by room temperature (313 K) adsorption.

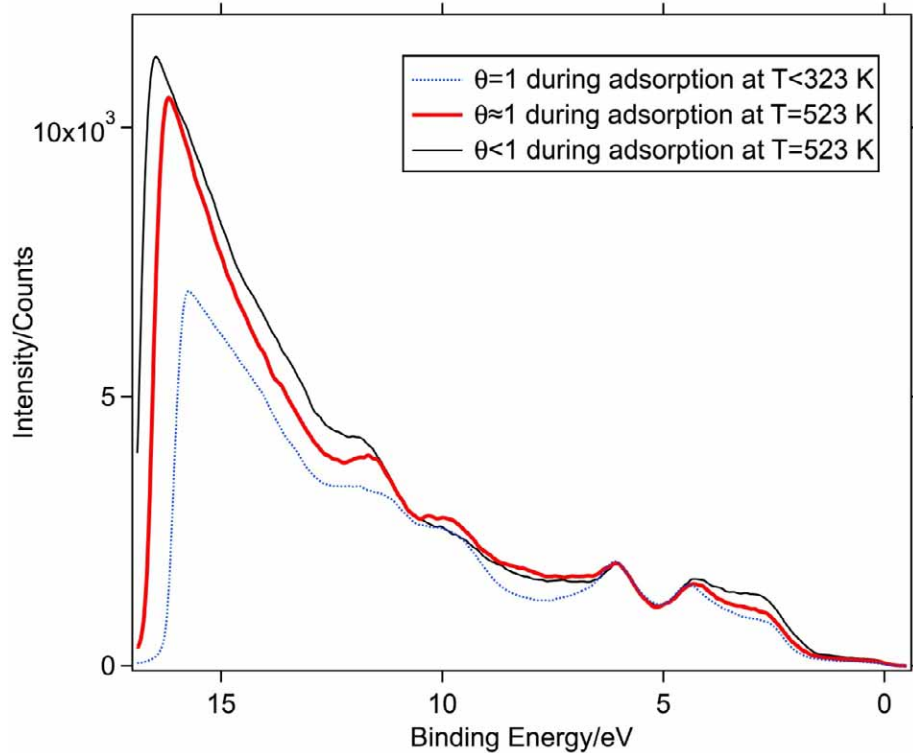


Figure SI 7. UP spectra for the  $(1\times 1)\text{-}\theta = 1$  and  $(1\times 3)\text{-}\theta < 1$  adsorption structures formed during adsorption at 523 K, and for the  $(1\times 1)\text{-}\theta = 1$  structure formed during adsorption at 313 K.

### The coulombic energy of one, two and three-dimensional ionic systems of finite size.

Here, for illustrative purposes, we choose  $n$  ions consisting of  $n/2$  positive ions and  $n/2$  negative ions arranged in particularly simple geometries. In one dimension the ions may be arranged as linear chains of alternating positive and negative ions; in two dimensions as a square chequer board array with alternate positive and negative ions; and in three dimensions as the rock-salt or NaCl structure which has alternate positive and negative ions in a cubic arrangement. In all of these the separation between positive and negative ions is  $r$ . Figure SI 8 shows linear chains of ions for  $n = 2, 4, 8, 12$  and  $16$ ; square and rectangular arrays for  $n = 4, 8, 12$  and  $16$  ions; and three dimensional cubic and rectangular parallelepiped arrays for  $n = 8$  and  $12$  ions.

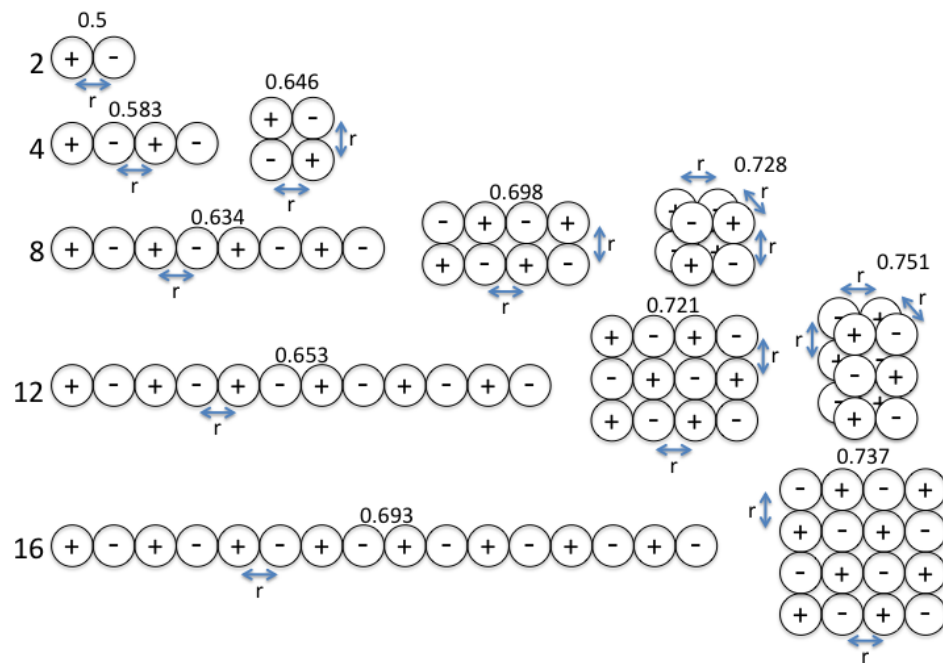


Figure SI 8. One and two-dimensional arrangements of positive and negative ions for totals of 2, 4, 8, 12 and 16 ions. Also shown are the three-dimensional arrangements for 8 and 12 ions. The number above each arrangement is the value of  $A$  per ion.

The coulombic interactions may be summed for each geometry giving the energy per ion,  $E/n$ , as

$$\frac{E}{n} = \frac{z_+ z_-}{4\pi\epsilon_0 r} A$$

where  $z_+$  and  $z_-$  are the charges on the ions (coulombs) and  $\epsilon_0$  is the permittivity of free space.  $A$  is a dimensionless constant which for systems of infinite size is the Madelung constant, which we shall also refer to as the Madelung constant for the systems of finite size considered here.  $A$  can be determined relatively quickly for small systems by manually summing the signed distances between all pairs of ions in units of  $r$ ; which was the (tedious) procedure adopted here. See refs 7-9 for more information on calculating Madelung constants. Figure SI 8 and the Table SI 1 shows values of  $A$  for 2, 4, 8, 12 and 16 ions (i.e. 1, 2, 4, 6 and 8 ion pairs) in the one, two and three-dimensional arrangements.

Table SI 1. Madelung constants for the one, two and three-dimensional systems shown in Fig. SI 8.

Number of ions	1 D	2D	3D
2	0.5		
4	0.583	0.646	
8	0.634	0.698	0.7280
12	0.653	0.721	0.751
16	0.663	0.737	-
$\infty$	0.693 = $\ln 2$	-	-

In one dimension, as the chains grows longer the value of  $A$ , and hence the coulomb energy per ion, increases tending to a limit of 0.693<sup>7</sup>. Similarly in two and three dimensions, as  $n$  increases so does  $A$  and the coulomb energy. It is also clear that for a given number of ions,  $n$ , the one dimensional arrangement is the least stable, followed by the two dimensional arrangement, with the three dimensional arrangement as the most stable. It follows that a linear array of  $n$  ions should spontaneously re-arrange itself into the lowest energy, three dimensional, arrangement. However, the transformation from one to three dimensions is not straightforward, as described in the main text of the paper.

## References

1. P. Marchand and L. Marmet, *Rev. Sci. Instrum.*, 1983, **54**, 1034-1041.
2. J. M. Gottfried, K. J. Schmidt, S. L. M. Schroeder and K. Christmann, *Surf. Sci.*, 2003, **536**, 206-224.
3. F. Evangelista, A. Ruocco, D. Pasca, C. Baldacchini, M. G. Betti, V. Corradini and C. Mariani, *Surf. Sci.*, 2004, **566**, 79-83.
4. F. Evangelista, A. Ruocco, V. Corradini, M. P. Donzello, C. Mariani and M. G. Betti, *Surf. Sci.*, 2003, **531**, 123-130.
5. H. L. Anderson, ed., *Physics Vade Mecum: a Physicist's Desk Reference*, 2nd edn., American Inst. of Physics, 1981.
6. O. Hofft, S. Bahr, M. Himmerlich, S. Krischok, J. A. Schaefer and V. Kempfer, *Langmuir*, 2006, **22**, 7120-7123.
7. C. Kittel, *Introduction to solid state physics*, 8th edn., John Wiley and Sons, Inc., 2005.
8. F. Seitz and D. Turnbull, eds., *Solid State Physics Vol. 16 Advances in Research and Applications*, Academic Press Inc., 1964.
9. F. C. Brown, *The Physics of Solids, Ionic Crystals, Lattice Vibrations, and Imperfections*, W.A. Benjamin Inc., 1967.